DEHUMIDIFICATION PERFORMANCE INVESTIGATION OF RUN-AROUND MEMBRANE ENERGY EXCHANGER SYSTEM

by

Miklos KASSAI[a]* Gaoming GE[b], and Carey J. SIMONSON[b]

[a] Budapest University of Technology and Economics, Budapest, Hungary
[b] University of Saskatchewan, Saskatoon, Sask., Canada

Original scientific paper
DOI: 10.2298/TSCI140816129K

Liquid-to-air membrane energy exchanger is a novel membrane base energy exchanger, which allows both heat and moisture transfer between air and a salt solution. It uses semi-permeable membrane to eliminate entrainment of liquid desiccant as aerosols in air stream and allow simultaneous heat and moisture transfer between salt solution flow and airflow. The heat and mass transfer performance of a single liquid-to-air membrane energy exchanger is significantly dependent on 2-D parameters. They are, the number of heat transfer units, and the ratio of heat capacity rates between solution flow and air flow (Cr). The liquid-to-air membrane energy exchangers can also be applied in a run-around membrane energy exchanger system, which is mainly comprised of two liquid-to-air membrane energy exchangers and a closed loop of aqueous desiccant solution and used as a passive energy recovery system to recover the energy (both heat and moisture) from the exhaust air to precondition the supply air in air conditioning systems. In this study the dehumidification capacity of a run-around membrane energy exchanger is investigated numerically at different exhaust air temperatures and Cr* values. Increasing the exhaust air temperature or the Cr* would enhance the dehumidification capacity of the a run-around membrane energy exchanger system under Cr* ≤ 1, but the improvement is limited. The dehumidification capacity at low Cr* is much lower than that under the optimal Cr* value (Cr* = 3.2) where the maximum latent effectiveness is obtained.*

Key words: *run-around membrane energy exchanger, dehumidification capacity, ventilation, energy efficiency*

Introduction

Heating, ventilating, and air conditioning systems (HVAC) are essential for the maintenance of a comfortable and healthy indoor environment for building occupants. In the field of sustainable building and its assessment, not only thermal comfort and indoor air quality, but also energy efficiency have been recognized as essential parameters of indoor environmental design [1]. In developed countries the HVAC systems consume around a third of the total energy consumption of the whole society. On the other hand, energy saving in buildings is being strictly regulated by official requirements and local authorities. Nowadays, the role of heat gains in the energy balance of a building is becoming more and more important. In a modern building, the ventilation losses may become more than 50% of total thermal loss-

* Corresponding author; e-mail: kas.miklos@gmail.com

es [2]. Taking into account the previous cited facts, the improvement of the efficiency in buildings ventilating systems in order to reduce their environmental impact constitutes a key issue [3, 4].

In the case of many buildings the 100% fresh air in HVAC systems results a significant increasing in the building cooling/heating loads [5, 6]. For such systems, it is necessary to use energy recovery systems to reduce this load. The operating objective of the energy recovery systems is to use the exhaust air of the room to pre-condition the outdoor air. By this way a substantial amount of energy is recovered which reduces the overall HVAC energy consumption. The development of energy recovery systems has led to improved performance and capability in recovering both sensible and latent energy [7]. Enthalpy energy exchangers that utilize a porous membrane as the heat and moisture transfer surface is one device that can recover both sensible and latent energy [8]. Energy recovery systems are commonly used in HVAC systems nowadays. They reduce the operation costs for conditioning ventilation air by both decreasing the required energy to the condition air and auxiliary energy consumption. Significant energy savings from these systems have been shown in several situations [9-11]. There are many types of energy recovery systems which are now cost effective in a wide range of ventilation designs. These systems include heat or enthalpy wheels, flat plate exchangers (heat/enthalpy), or run-around glycol loops. The operation and performance of these systems is well described in literature [12]. The liquid-to-air membrane energy exchanger (LAMEE) is a new membrane-based liquid desiccant device, which uses semi-permeable membranes to eliminate entrainment of liquid desiccant as aerosols in air stream and allow simultaneous heat and moisture transfer between salt solution flow and airflow. The LAMEE exchangers can be used as air dehumidifiers for supply air or desiccant solution regenerators in liquid desiccant air conditioning systems. Over the past years, the performance of single LAMEE has been comprehensively studied, including the steady-state effectiveness [13-15] and transient performance [16, 17] under different operating conditions (*e. g.* air dehumidification and solution regeneration conditions). Up to 95% total effectiveness for the single LAMEE can be achieved, and its effectiveness (sensible, latent, and total) increases as the number of heat transfer units (*NTU*) and Cr^* values increase [18].

The LAMEE can also be applied in a run-around membrane energy exchanger (RAMEE) system, which is mainly comprised of two LAMEE, and a closed loop of aqueous desiccant solution and used as a passive energy recovery system to recover the energy (both heat and moisture) from the exhaust air to precondition the supply air in air conditioning systems [19]. The steady-state and transient effectiveness as well as energy savings potential of RAMEE systems have been experimentally measured and numerically simulated [20-25]. Early test results showed that a 55% total effectiveness could be achieved by RAMEE systems using two laboratory-constructed counter-cross-flow LAMEE for energy recovery from the exhaust air (*i. e.* higher than the minimum total effectiveness 50% required by ASHRAE Standard 90 [26]. In the RAMEE system, the effectiveness always increases as the *NTU* value increases, while the effectiveness increases with Cr^* at lower Cr^* values until it reaches the peak value, after which the effectiveness decreases as the Cr^* increases. The optimal Cr^* is dependent on the operating condition (*i. e.* outdoor air state) and the heat and mass transfer performance of the system. For example, the maximum total effectiveness of a RAMEE system in our previous study was achieved at $Cr^* = 1.5$ and 2.5 in Air-Conditioning, Heating and Refrigeration Institute (AHRI) winter and summer test conditions, respectively [27]. Using hourly simulations for an office building and a hospital building in four different North American cities, Rasouli *et al.* [28, 29] and Rasouli [30] found that a RAMEE provided up to 40-

60% annual heating energy saving and up to 20% annual cooling energy saving in the office and hospital buildings, respectively, depending on the climate and RAMEE effectiveness. The life-cycle cost analysis showed that the payback period of the energy recovery ventilator (ERV) was within two years in cold climates and 1-5 years in hot climates. The payback period of ERV was about two years sooner for the hospital building than in the office building [30]. This difference is caused mostly by the higher ventilation rates required for a hospital.

Working principle of the RAMEE system is, more or less, similar to the energy wheel which is a well-developed and widely applied energy recovery device in building HVAC systems. The energy wheel rotates slowly (*i. e.* 20~30 r/min.), within the supply and exhaust air streams and recovers energy from the exhaust air. When the exhaust air is heated (*i. e.* 70~80 °C or even higher), and rotation speed is reduced (*i. e.* 3~5 r/min.), the dehumidification capacity of the wheel increases substantially [31]. The wheel is commonly defined as desiccant wheel in these operating conditions, and it is mainly used to dry air flow. Similarly, the impacts of exhaust air temperatures and Cr^* values (*i. e.* desiccant solution flow rates) on the dehumidification capacity of a RAMEE system are numerically investigated under low Cr^* values ($Cr^* \leq 1$) in this study.

Liquid-to-air membrane energy exchanger

The LAMEE is a flat-plate energy exchanger constructed with multiple air and liquid flow channels each separated by a semi-permeable membrane, which is permeable to water vapor but impermeable to liquid water. In this study, a small-scale single-panel LAMEE with a counter-cross-flow configuration for air and solution flows is tested during dehumidification operating conditions. The small-scale single-panel LAMEE was designed to minimize the sources of errors in LAMEE performance evaluation, and facilitate research and development of LAMEE by saving the money and time. The LiCl solution flows from top to bottom in the small-scale LAMEE. Figure 1 shows the air and solution flow configurations of the tested LAMEE. Two grooved plastic liquid-flow panels are each enclosed by a semi-permeable membrane to form two solution channels, one on each side of the air channel. An air spacer is used to form an air channel of constant thickness. The small-scale liquid-to-air membrane energy exchanger specifications and membrane properties are presented in tab. 1.

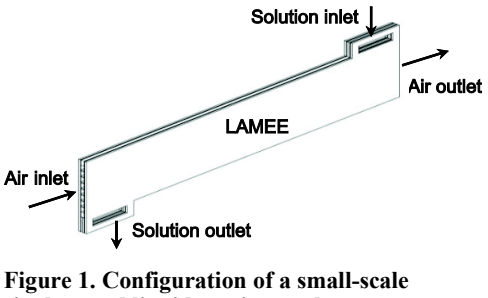

Figure 1. Configuration of a small-scale single-panel liquid-to-air membrane energy exchanger [27]

Table 1. Specifications and membrane properties of the small-scale liquid-to-air membrane energy exchanger [27]

Parameter	Value
Exchanger length, [m]	0.99
Exchanger aspect ratio of the air-liquid contact area, [–]	10.5
Exchanger entrance ratio, [–]	0.025
Air gap thickness, [mm]	5
Solution gap thickness in each side panel, [mm]	1.2
Water vapor transmission resistance of membrane, [sm^{-1}]	24
Membrane thermal conductivity, [$Wm^{-1}K^{-1}$]	0.065
Membrane thickness, [mm]	0.265

Run-around membrane energy exchanger

Run-around membrane energy exchanger system

A RAMEE system is comprised of two or more separated LAMEE and an aqueous desiccant solution (in this research LiCl, solution) that is pumped in a closed loop between the LAMEE, as shown in fig. 2. In a typical RAMEE system, one LAMEE is located in the outdoor supply air stream entering the building, and another LAMEE is located in the exhaust air stream leaving the building. Heat and moisture are transferred between the air and desiccant solution through the membrane in each LAMEE. As a consequence, the RAMEE system passively recovers energy from the exhaust air to precondition the supply air in the air conditioning system.

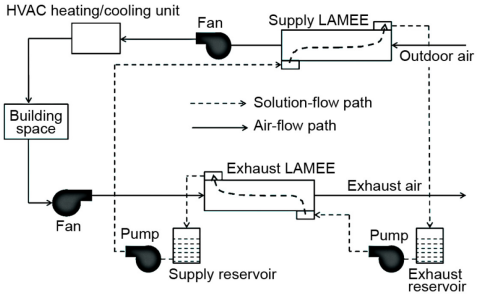

Figure 2. Schematic of a counter-cross-flow run-around membrane energy exchanger [23]

Performance factors

The heat and mass transfer performance of a single LAMEE or a RAMEE is significantly dependent on 2-D parameters. They are the *NTU* and the ratio of heat capacity rates between solution flow and air flow, *Cr**, as defined by eqs. (1) and (2) [32]:

$$NTU = \max\left\{\frac{2UA}{C_{\text{air}}}, \frac{2UA}{C_{\text{sol}}}\right\} \tag{1}$$

$$Cr^* = \frac{C_{\min}}{C_{\text{air}}} = \frac{\dot{m}_{\min} c_{p,\min}}{\dot{m}_{\text{air}} c_{p,\text{air}}} \tag{2}$$

where A is the membrane surface area, C – the heat capacity rate, $\dot{m}$ – the mass flow rate, and c_p – the specific heat capacity.

Additionally, if $Cr^* \geq 1$, then $(\dot{m}c_p)_{\min} = \dot{m}_{\text{air}} c_{p,\text{air}}$. If $Cr^* < 1$, then $(\dot{m}c_p)_{\min} = \dot{m}_{\text{sol}} c_{p,\text{sol}}$, where subscripts air and sol represent the air stream and solution flow, respectively.

For a RAMEE system, the definition of effectiveness is similar to the single LAMEE, but the inlet desiccant solution state is replaced by the corresponding inlet state of exhaust air. The effectiveness of the supply and exhaust exchangers are calculated by eqs. (3) and (4), respectively. The overall effectiveness of the RAMEE system is the average value of these two exchangers under steady-state, as shown in eq. (5).

$$\varepsilon_{X,\text{sup}} = \frac{\dot{m}_{\text{air}} c_{p,\text{air}}}{(\dot{m}c_p)_{\min}} \frac{X_{\text{air,in,sup}} - X_{\text{air,out,sup}}}{X_{\text{air,in,sup}} - X_{\text{air,in,exh}}} \tag{3}$$

$$\varepsilon_{X,\text{exh}} = \frac{\dot{m}_{\text{air}} c_{p,\text{air}}}{(\dot{m}c_p)_{\min}} \frac{X_{\text{air,out,exh}} - X_{\text{air,in,exh}}}{X_{\text{air,in,sup}} - X_{\text{air,in,exh}}} \tag{4}$$

$$\varepsilon_{o,X} = \frac{\varepsilon_{X,\text{sup}} + \varepsilon_{X,\text{exh}}}{2} \tag{5}$$

where $\varepsilon_{X,\text{sup}}$, $\varepsilon_{X,\text{exh}}$, and $\varepsilon_{o,X}$, represent sensible and latent effectiveness of the supply LAMEE exhaust LAMEE, and the whole RAMEE system, respectively, X represents the air temperature, moisture content or enthalpy values [32].

Dehumidification performance of a run-around membrane energy exchanger at low *Cr** conditions

Numerical modeling of a run-around membrane energy exchanger

The validated numerical model of a single LAMEE can also be used to predict the performance of a RAMEE system when $Cr^* < 1$. By coupling two LAMEE in a closed loop, the numerical model can simulate the steady-state energy performance of a RAMEE system after enough iterations (*e. g.* > 5000 iterations). The energy performance (*i. e.* effectiveness) of a RAMEE system at low *Cr** conditions would be estimated using numerical model.

An enthalpy pump system (EPS) code is used to numerically evaluate the performance of the small-scale LAMEE. The EPS code has been developed by the University of Saskatchewan RAMEE research group [27] and is modified based on the geometry and specifications of the small-scale single-panel LAMEE.

Some simplifying assumptions are made to reduce the complexity of the calculation process. These assumptions, which do not significantly affect the accuracy of the model, are:

– the fluid flows in each exchanger are 1-D and counter flow,
– the heat and mass transfer processes occur only normal to each membrane and the membrane properties are constant and steady-state,
– axial heat conduction and water molecular diffusion in the two fluids in the flow directions are negligible, and
– phase change heat gain or loss due to adsorption/desorption of water vapor at the membrane surface occurs only on the liquid side.

Based on the previous assumptions, the steady-state governing equation for coupled heat and moisture transfer for each fluid in a LAMEE are [32]:

$$\frac{\dot{m}_{\text{air}}}{H} c_{p,\text{air}} \frac{\mathrm{d}T_{\text{air}}}{\mathrm{d}x} + 2U(T_{\text{air}} - T_{\text{sol}}) = 0 \tag{6}$$

$$\frac{\dot{m}_{\text{sol}}}{H} c_{p,\text{sol}} \frac{\mathrm{d}T_{\text{sol}}}{\mathrm{d}x} - 2U_{\text{m}}(W_{\text{air}} - W_{\text{sol}})h_{fc} - 2U(T_{\text{air}} - T_{\text{sol}}) = 0 \tag{7}$$

$$\frac{\dot{m}_{\text{air}}}{H} \frac{\mathrm{d}W_{\text{air}}}{\mathrm{d}x} + 2U(W_{\text{air}} - W_{\text{sol}}) = 0 \tag{8}$$

$$\frac{\dot{m}_{\text{sol}}}{H} \frac{\mathrm{d}X_{\text{sol}}}{\mathrm{d}x} - 2U_{\text{m}}(W_{\text{air}} - W_{\text{sol}}) = 0 \tag{9}$$

where $\dot{m}_{\text{air}}$ and $\dot{m}_{\text{sol}}$ are the mass flow rates of dry air and salt solution through a single channel, respectively, H – the height of energy exchanger, and U and U_{m} – the overall heat and mass transfer coefficients between the air and salt solution, respectively. They are obtained from eqs. (10) and (11) [32]:

$$U = \left(\frac{1}{h_{\text{sol}}} + \frac{\delta}{k} + \frac{1}{h_{\text{air}}} \right)^{-1} \tag{10}$$

$$U_{\mathrm{m}} = \left(\frac{1}{h_{\mathrm{m,\,air}}} + \frac{\delta}{k_{\mathrm{m}}} \right)^{-1} \tag{11}$$

where h_{sol} and h_{air} are the convective heat transfer coefficients of the desiccant solution flow and the air flow, respectively, k – the thermal conductivity of the membrane separating the two fluid streams, $h_{\mathrm{m,air}}$ – the convective mass transfer coefficient of the air stream, k_{m} – the permeability of the membrane, and δ – the thickness of the membrane. Hemingson [24] has shown that $h_{\mathrm{m}\,sol} \gg h_{\mathrm{m,air}}$ so the resistance to moisture transfer in the solution channel can be neglected in eq. (11).

Furthermore, the analytical latent effectiveness of the small-scale LAMEE is calculated based on a heat and mass transfer analogy from this analytical model [33]. The heat and mass transfer analogy is given by the following correlation [33]:

$$\mathrm{Sh} = \mathrm{Nu}\ \mathrm{Le}^{-1/3} \tag{12}$$

where Sh, Nu, and Le are the Sherwood, Nusselt, and Lewis dimensionless groups. The convective heat and mass transfer coefficients are found from the Nusselt and Sherwood number definitions [34]:

$$\mathrm{Nu} = \frac{hD_{\mathrm{h}}}{k_{\mathrm{f}}} \tag{13}$$

$$\mathrm{Sh} = \frac{h_{\mathrm{m}} D_{\mathrm{h}}}{D_{\mathrm{v-a}}} \tag{14}$$

where k_{f} [$\mathrm{Wm^{-1}K^{-1}}$] is the thermal conductivity of the fluid, h_{m} – the convective mass transfer coefficient, and D_{h} and $D_{\mathrm{v\text{-}a}}$ – the hydraulic diameter and diffusivity coefficient of vapor into air, respectively. By substituting the equation for Sherwood and Nusselt numbers into eq. (12), the convective mass transfer coefficient for air and solution is found:

$$h_{\mathrm{m}} = \frac{h}{c_p}\ \mathrm{Le}^{-2/3} \tag{15}$$

where c_p [$\mathrm{Jkg^{-1}K^{-1}}$] is the specific heat capacity, Le – the Lewis number which is defined as the ratio between the thermal to mass diffusivities [35].

It should be mentioned that the values of Nusselt and Sherwool numbers are important in the special membrane-based liquid-to-air energy exchangers, which are used to calculate the convective heat and mass transfer coefficients (*i. e.* h_{c} and h_{m}) in the exchangers. In this study, we assume the heat flux through the membrane is constant in the counter-cross-flow LAMEE. Actually, this assumption agrees well with what Zhang *et al.* [36] found for the counter-flow hollow fiber liquid desiccant dehumidifier, where the $\mathrm{Nu_C}$ was very close to $\mathrm{Nu_H}$. Under this assumption (*i. e.* constant heat flux), the actual Nusselt number for the air side of the LAMEE was experimentally measured in the wind tunnel energy exchanger insert test facility, as shown in our previous paper [15]. For the solution side, due to the $\mathrm{Re_{sol}}$ is very low (around 20) and L/δ = 825, where L is the length and δ the solution gap thickness of membrane, respectively. Consequently, the Nusselt number ($\mathrm{Nu_{sol}}$ = 5.39) for laminar flow between two infinite parallel plates with constant heat flux on both wall is used for the solu-

tion flow. The Nusselt number value is then used to calculate the convective heat transfer coefficient using eq. (13).

The LAMEE latent effectiveness values for counter, cross and counter-cross flow exchangers are calculated by eqs. (16)-(18) [37]:

$$\varepsilon_{\text{latent,cross}} = 1 - \exp\left\{\frac{NTU_{\text{m}}^{0.22}}{m^*}\left[\exp(-m^* NTU_{\text{m}}^{0.78}) - 1\right]\right\} \tag{16}$$

$$\varepsilon_{\text{latent,counter}} = \frac{1 - \exp[-NTU_{\text{m}}(1 - m^*)]}{1 - m^* \exp[-NTU_{\text{m}}(1 - m^*)]} \tag{17}$$

$$\varepsilon_{\text{latent}} = \frac{A_{\text{cross}}}{A}\varepsilon_{\text{latent,cross}} + \frac{A_{\text{counter}}}{A}\varepsilon_{\text{latent,counter}} \tag{18}$$

where the dimensionless groups NTU_{m} and m^* are the number of mass transfer units and mass flow rate ratio, respectively. The heat and mass transfer problems are uncoupled in this analytical model using the heat and mass transfer analogy where the latent effectiveness is found based on sensible effectiveness correlation and substituting the NTU and Cr^* with NTU_{m} and m^* are calculated for the LAMEE system:

$$NTU_m = \frac{U_{\text{m}} A}{\dot{m}_{\min}} = \frac{U_{\text{m}} A}{\dot{m}_{\text{air}}} \tag{19}$$

$$m^* = \frac{\dot{m}_{\min}}{\dot{m}_{\max}} = \frac{\dot{m}_{\text{air}}}{\dot{m}_{\text{sol}}} \tag{20}$$

$$U_{\text{m}} = \left(\frac{1}{h_{\text{m,air}}} + R_{\text{mem}} + \frac{1}{h_{\text{m,sol}}}\right)^{-1} \tag{21}$$

where U_{m} is the overall convective mass transfer coefficient, and R_{mem} – the membrane moisture transfer resistance.

Table 2. The AHRI inlet air conditions for run-around membrane energy exchanger performance tests in summer [38]

Summer	$T_{\text{air,in,sup}}$	308.15 K (35 °C)
	$W_{\text{air,in,sup}}$	17.5 g/kg (50% RH)
	$T_{\text{air,in,exh}}$	297.15 K (24 °C)
	$W_{\text{air,in,exh}}$	9.3 g/kg (50% RH)

In the numerical simulations, the AHRI summer condition (tab. 2) is adopted as the basic test condition for the RAMEE system. The exhaust air temperature, $T_{\text{air,in,exh}}$, is increased from 24 °C to 48 °C with an interval of 6 °C. It should be mentioned that crystallization of desiccant solution may occur in the RAMEE system when the $T_{\text{air,in,exh}}$ is higher than 51 °C, since the relative humidity (RH) of exhaust air is lower than 11% in the conditions. The supply air outlet humidity ratios are evaluated under different operating conditions with different Cr^* values (Cr^* = 0.5-1.0) and a constant NTU value (NTU = 10) in the RAMEE system. During our research LiCl salt solution was used. The solution inlet temperature was 22.8 °C and concentration of it was 35%. Based on previous research results with RAMEE, NTU = 10 showed an optimal value taking into account value of the effectiveness [19]. The steady-state simulation results are presented in the following section.

Dehumidification performance of the run-around membrane energy exchanger

The supply air outlet humidity ratios ($W_{air,out,sup}$) under different operating conditions under steady-state simulations are show in fig. 3(a) when $Cr^* \leq 1$. It can be found that the supply air outlet humidity ratio decreases as the Cr^* increases at different exhausted air temperatures, except $T_{air,in,exh} = 48$ °C, where the $W_{air,out,sup}$ is almost constant. It means that the air dehumidification capacity increases when the solution flow rate increases. Correspondingly, the latent effectiveness of the RAMEE system increases with the Cr^* at lower values, as shown in fig. 3(b). These results are consistent to our previous findings, where the latent effectiveness increases with Cr^* at lower Cr^* values until it reaches the peak value [19].

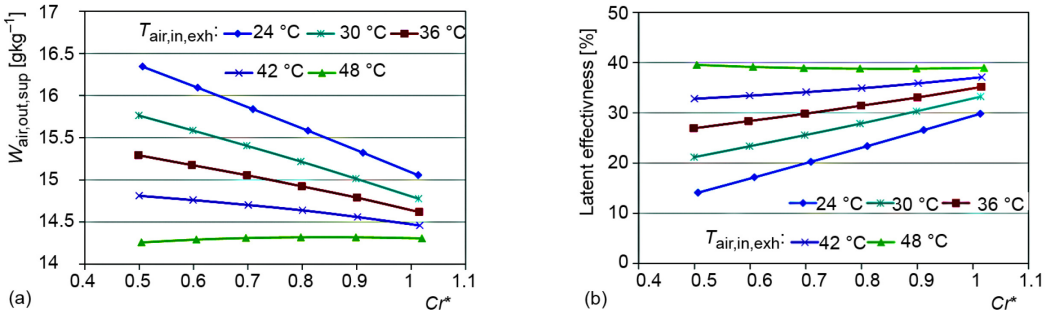

Figure 3. (a) The supply air outlet humidity ratio, and (b) latent effectiveness of the run-around membrane energy exchanger at different low Cr^* conditions ($NTU = 10$, $0.5 \leq Cr^* \leq 1$)

Additionally, as the exhaust air temperature increases, the supply air outlet humidity ratio decreases. The reason is that the solution regeneration process in the exhaust LAMEE (or regenerator) is enhanced when the exhaust air temperature increases, consequently the solution concentration increases. It would improve the air dehumidification capacity of the supply LAMEE (or dehumidifier).

The supply air outlet humidity ratio and latent effectiveness of the RAMEE system at different Cr^* conditions, including both $Cr^* \leq 1$ and $Cr^* > 1$ conditions, are presented in fig. 4. It can be seen that the supply air outlet humidity ratio decreases firstly and then increa-

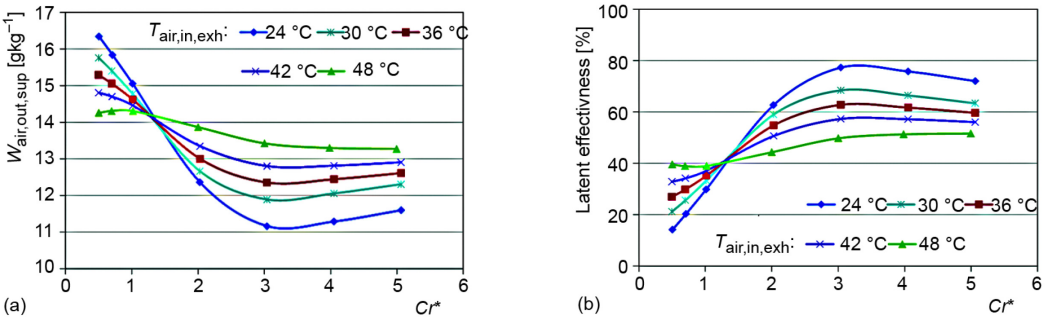

Figure 4. (a) The supply air outlet humidity ratio and (b) latent effectiveness of the run-around membrane energy exchanger at different Cr^* conditions ($NTU = 10$, $0.5 \leq Cr^* \leq 5$)

ases a little bit as the *Cr** changes in the range of 0.5-5. Correspondingly, the latent effectiveness of the RAMEE system increases with *Cr** at lower *Cr** values until it reaches the peak value, after which the effectiveness decreases as the *Cr** increases. The optimal *Cr** value is around 3.2 for the tested RAMEE system during the simulated conditions.

Moreover, fig. 4(a) shows that the supply air outlet humidity ratio decreases as the exhaust air temperature increases in the range of $Cr^* \leq 1$, which is opposite to that of $Cr^* > 1$. When $Cr^* > 1$, the higher the exhaust air temperature, the higher the supply air outlet humidity ratio; while $Cr^* \leq 1$, the higher the exhaust air temperature, the lower the supply air outlet humidity ratio. The reason is that the temperature of desiccant solution entering the supply LAMEE is higher in the RAMEE system as the exhaust air temperature increases. In the range of $Cr^* > 1$, although the solution concentration also increases a little with the increasing solution temperature, the overall dehumidification capacity of the supply LAMEE decreases consequently.

According to the simulation results, it is found that the maximum dehumidification capacity of the RAMEE system is achieved at $Cr^* = 3.2$ when the exhaust air temperature is 24 °C. When $Cr^* > 1$, the latent effectiveness and air dehumidification capacity of RAMEE decrease substantially as the exhaust air temperature increases; when $Cr^* \leq 1$, increasing the exhaust air temperature can enhance the air dehumidification capacity. However, this enhancement is quite limited. Obviously, it is not a good method to improve the supply air dehumidification capacity of a RAMEE system by heating the exhaust air flow. In fact, the RAMEE systems can achieve good dehumidification capacities under proper operating condition (*i. e.* the optimal *Cr** condition) by passive energy (both heat and moisture) recovery in the air-conditioning systems. Comparing the results with a previous research with RAMEE by Mahmud [39], higher latent effectiveness can be achieved using LiCl than with $MgCl_2$ desiccant solution. The result showed that the difference can be 30% higher with LiCl operation in the case of AHRI summer test conditions. In addition, cooling the desiccant solution which enters the supply LAMEE is a cost-efficient method to improve the system dehumidification capacity in active liquid desiccant air-conditioning systems, which has been verified in our previous study [18].

Conclusion

The impacts of exhaust air temperatures and *Cr** values on the supply air outlet humidity ratio in a RAMEE system are numerically investigated in this research. When $Cr^* \leq 1$, increasing the solution flow rate (*i. e. Cr** value) or the exhaust air temperature would enhance the dehumidification capacity of the RAMEE system, but the improvement is limited; while $Cr^* > 1$, increasing the exhaust air temperature would substantially reduce the dehumidification capacity of the RAMEE. Heating the exhaust air flow is not recommended to enhance the supply air dehumidification capacity of RAMEE systems. Proper operation of RAMEE systems (*i. e.* under the optimal *Cr** condition) during passive energy recovery or actively cooling the desiccant solution entering the supply LAMEE can achieve good dehumidification capacity in the liquid desiccant air-conditioning systems.

Acknowledgments

This research was financially supported by the Natural Science and Engineering Research Council of Canada (NSERC) and Venmar CES, Inc., Saskatoon, Sask., Canada and Hungarian Eotvos Scholarship, Balassi Institute – Hungarian Scholarship Board Office, Budapest, Hungary.

Nomenclature

A – surface area of membrane, [m^2]
C – heat capacity rate, [kWK^{-1}]
Cr^* – ratio of heat capacity rates (solution/air)
c_p – specific heat capacity, [$Jkg^{-1}\ K^{-1}$]
D_h – hydraulic diameter based on channel thickness, [mm]
D_{v-a} – diffusivity coefficient of vapor into air, [m^2s^{-1}]
H – height of energy exchanger, [m], or enthalpy, [Jkg^{-1}]
h – convective heat transfer coefficient, [$Wm^{-2}s^{-1}$]
h_{fc} – net heat of phase change, [Jkg^{-1}]
h_m – convective mass transfer coefficient, [$kgm^{-2}\ s^{-1}$]
k_f – thermal conductivity of the fluid, [$Wm^{-1}K^{-1}$]
k_m – permeability of the membrane, [$kgms^{-1}$]
Le – Lewis number, [–]
$\dot{m}$ – mass flow rate, [kgs^{-1}]
m^* – mass flow rate ratio, [–]
Nu – Nusselt number, [–]
NTU – number of heat transfer units, [–]
NTU_m – number of mass transfer units, [–]
Re – Reynolds number, [–]
RH – relative humidity
Sh – Sherwood number, [–]
T – temperature, [K]
U – overall heat transfer coefficient, [$Wm^{-2}\ K^{-1}$]
U_m – overall mass transfer coefficient, [$kgm^{-2}\ s^{-1}$]
W – humidity ratio, [$kgkg_{air}^{-1}$]
X – ratio of water mass to mass of pure salt, [$kgkg^{-1}$]

Greek symbols

δ – thickness of the membrane [mm]
ε – effectiveness [–]

Subscripts

air – air side
C – uniform heat flux boundary condition
exh – exhaust air
in – inlet
H – uniform heat flux boundary condition
out – outlet
sol – salt solution
sup – supply air

References

[1] Fan, Y., Ito, K., Energy Consumption Analysis Intended for Real Office Space with Energy Recovery Ventilator by Integrating BES and CFD Approaches, *Building and Environment, 52* (2012), June, pp. 57-67
[2] Zhang, L.-Z., *et al.*, Heat and Moisture Transfer in application Scale Parallel-Plates Enthalpy Exchangers with Novel Membrane Materials, *Journal of Membrane Science, 325* (2008), 2, pp. 672-682
[3] Fehrm, M., *et al.*, Exhaust Air Heat Recovery in Buildings, *International Journal of Refrigeration, 25* (2002), 4, pp. 439-449
[4] Ignjatović, M. G., *et al.*, Influence of Glazing Types and Ventilation Principles in Double Skin Facades on Delivered Heating and Cooling Energy During Heating Season in an Office Building, *Thermal Science*, *16* (2012), 2, pp. 461-469
[5] Nguyen, A., *et al.*, Experimental Study of Sensible Heat Recovery of Heat Pump During Heating and Ventilation, *International Journal of Refrigeration, 28* (2005), 2, pp. 242-252
[6] Zhang, L.-Z., Energy Performance of Independent Air Dehumidification Systems with Energy Recovery Measures, *Energy, 31* (2006), 8-9, pp. 1228-1242
[7] Zhang, L.-Z, Thermodynamic Modelling of a Novel Air Dehumidification System, *Energy and Buildings, 37* (2005), 3, pp. 279-286
[8] Nasif, M., *et al.,* Membrane Heat Exchanger in HVAC Energy Recovery Systems, Systems Energy Analysis, *Energy and Buildings, 42* (2010), 10, pp. 1833-1840
[9] Zhang, L.-Z, Niu, J. L., Energy Requirements for Conditioning Fresh Air and the Long-Term Savings with a Membrane-Based Energy Recovery Ventilator in Hong Kong, *Energy, 26* (2002), 2, pp. 119-135
[10] Zhou, Y. P., *et al.*, Performance of Energy Recovery Ventilator with Various Weathers and Temperature Set-Points, *Energy and Buildings, 39* (2006), 12, pp. 1202-1210
[11] Šumarac, D. M., *et al.*, Energy Efficiency of Residential Buildings in Serbia, *Thermal Science*, *14* (2010), Suppl. 1, pp. S97-S113
[12] Zhang, L.-Z, Niu, J. L., Performance Comparisons of Desiccant Wheels for Air Dehumidification and Enthalpy Recovery, *Applied Thermal Engineering, 22* (2002), 12, pp. 1347-1367

[13] Moghadamm, D. G., *et al.*, Small-Scale Single-Panel Liquid-to-Air Membrane Energy Exchanger (LAMEE) Test Facility Development, Commissioning and Evaluating the Steady-State Performance, *Energy and Buildings, 66* (2013), Nov., pp. 424-436
[14] Ge, G., *et al.*, Comparison of Experimental Data and a Model for Heat and Mass Transfer Performance of a Liquid-to-Air Membrane Energy Exchanger (LAMEE) when Used for Air Dehumidification and Salt Solution Regeneration, *International Journal of Heat and Mass Transfer, 68* (2014), Jan., pp. 119-131
[15] Moghadamm, D. G., *et al.*, Numerical Model of a Small-Scale Liquid-to-Air Membrane Energy Exchanger: Parametric Study of Membrane Resistance and Air Side Convective Heat Transfer Coefficient, *Applied Thermal Engineering, 61* (2013), 2, pp. 245-258
[16] Namrav, R., *et al.*, Transient Characteristics of a Liquid-to-Air Membrane Energy Exchanger (LAMEE) Experimental Data with Correlations, *International Journal of Heat and Mass Transfer, 55* (2012), 23, pp. 6682–6694
[17] Namrav, R., *et al.*, Transient Heat and Moisture Transfer Characteristics of a Liquid-to-Air Membrane Energy Exchanger (LAMEE) Model Verification and Extrapolation, *International Journal of Heat and Mass Transfer, 66* (2013), Nov., pp. 757-771
[18] Abdel-Salam, A. H., *et al.*, Performance Analysis of a Membrane Liquid Desiccant Air-Conditioning System, *Energy and Buildings, 62* (2013), July, pp. 559-569, DOI: 10.1016/j.enbuild.2013.03.028
[19] Ge, G., *et al.*, Research and Applications of Liquid-to-Air Membrane Energy Exchangers in Building HVAC Systems at University of Saskatchewan: A review, *Renewable and Sustainable Energy Reviews, 26* (2013), Oct., pp. 464-479
[20] Erb, B., *et al.*, Experimental Measurements of a Run-Around Membrane Energy Exchanger with Comparison to a Numerical Model, *ASHRAE Transactions*, *115* (2009), 2, pp. 689-705
[21] Seyed-Ahmadi, M., *et al.*, Transient Behavior of Run-Around Heat and Moisture Exchanger System, Part I: Model Formulation and Verification, *International Journal of Heat and Mass Transfer, 52* (2009), 25, pp. 6000-6011
[22] Seyed-Ahmadi, M., *et al.*, Transient Behavior of Run-Around Heat and Moisture Exchanger System. Part II: Sensitivity Studies for a Range of Initial Conditions, *International Journal of Heat and Mass Transfer, 52* (2009), 26, pp. 6012-6020
[23] Mahmud, K., *et al.*, Performance Testing of a Counter-Cross-Flow Run-Around Membrane Energy Exchanger (RAMEE) System for HVAC Applications, *Energy and Buildings,* 42 (2010), 7, pp. 1139-1147
[24] Hemingson, H. B., The Impacts of Outdoor Air Conditions and Non-Uniform Exchanger Channels on a Run-Around Membrane Energy Exchanger, M. Sc. thesis, University of Saskatchewan, Saskatoon, Saskatchewan, Canada, 2010
[25] Vali, A., *et al.*, Numerical Model and Effectiveness Correlations for a Run-Around Heat Recovery System with Combined Counter and Cross Flow Exchangers, *International Journal of Heat and Mass Transfer, 52* (2009), 25, pp. 5827-5840
[26] ***, ANSI/ASHRAE Standard (American Society of Heating, Refrigerating, and Air-Conditioning Engineers) 90.1-2007, Energy Standard for Buildings Except for Low-rise Residential Buildings, Atlanta, Geo., USA, 2007
[27] Moghadamm, D. G., *et al.*, Evaluating the Steady-State Performance of a Small-Scale Single-Panel Liquid-to-Air Membrane Energy Exchanger (LAMEE) Under Summer AHRI Test Condition, *Proceedings*, 11th REHVA World Congress & 8th International Conference on IAQVEC, Prague, Czech Republic, 2013
[28] Rasouli, M., *et al.*, Application of a Run-Around Membrane Energy Exchanger in an Office Building HVAC System, *ASHRAE Transactions, 117,* (2011), 2, pp. 686-703
[29] Rasouli, M., *et al.*, Applicability and Optimum Control Strategy of Energy Recovery Ventilators in Different Climatic Conditions, *Energy and Buildings, 42,* (2010), 9, pp. 1376-1385
[30] Rasouli, M., Building Energy Simulation of a Run-Around Membrane Energy Exchanger (RAMEE), M. Sc. thesis, University of Saskatchewan, Saskatoon, Saskatchewan, Canada, 2010
[31] Simonson, C. J., *et al.*, Determining the Performance of Energy Wheels: Part I-Experimental and Numerical Method, *ASHRAE Transactions*, *105* (1999), 4243(RP-862)
[32] Ge, G., *et al.*, Analytical Model Based Performance Evaluation, Sizing and Coupling Flow Optimization of Liquid Desiccant Run-Around Membrane Energy Exchanger Systems, *Energy and Buildings, 62* (2013), July, pp. 248-257

[33] Niu, J. L., *et al.*, Membrane-Based Enthalpy Exchanger: Material Consideration and Clarification of Moisture Resistance, *Journal of Membrane Science, 189* (2001), 2, pp. 179-191
[34] Zhang, L.-Z., An Analytical Solution to Heat and Mass Transfer in Hollow Fiber Membrane Contactors for Liquid Desiccant Air Dehumidification, *ASME Journal of Heat Transfer, 133* (2011), 9, pp. 1-8
[35] Welty, J. R., *et al.*, *Fundamentals of Momentum, Heat, and Mass Transfer*, John Wiley & Sons Inc., New York, USA, 2001
[36] Zhang, L.-Z., *et al.*, Conjugate Heat and Mass Transfer in a Hollow Fiber Membrane Module for Liquid Desiccant air Dehumidification: a Free Surface Model Approach, *International Journal of Heat and Mass Transfer, 55*, (2012), 13, pp. 3789-3799
[37] Morrison, M. S., *et al.*, Heat and Mass Transfer in Air to Air Enthalpy Heat Exchangers, *Proceedings,* 6th International Conference on Heat Transfer, Fluid Mechanics and Thermodynamics, Matsushima, Japan, 2005
[38] ***, ANSI/AHRI Standard 1060 (I-P). Performance Rating of Air-to-Air Heat Exchangers for Energy Recovery Ventilation Equipment, Arlington, Va., USA, 2011
[39] Mahmud, K., Design and Performance Testing of Counter-Cross-Flow Run-Around Membrane Energy Exchanger System, M. Sc. thesis, University of Saskatchewan, Saskatoon, Saskatchewan, Canada, 2009

Paper submitted: August 16, 2014
Paper revised: October 2, 2014
Paper accepted: November 3, 2014